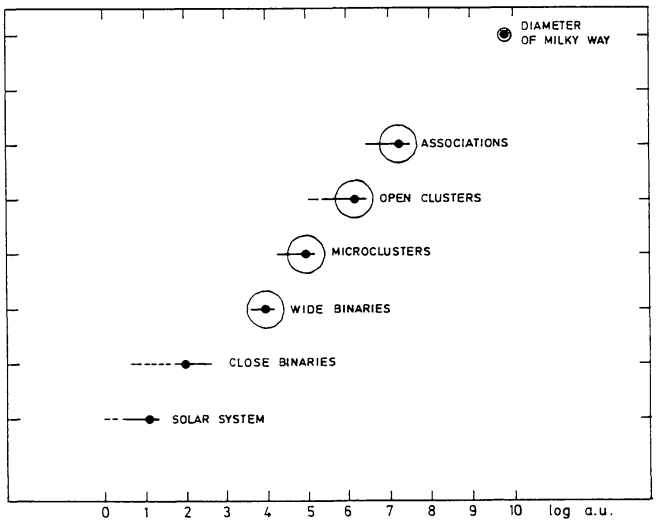

Fig. 1. If various types of stellar agglomerations in the Milky Way are arranged according to their typical linear dimensions we obtain this picture which has a certain pedagogic value, although its physical importance is debatable. The encircled objects represent the probable indicators of star-forming regions and the intention is to give an idea about the extension of such regions.

ABUNDANCES OF CLASSICAL CEPHEIDS AND EVIDENCE FOR SECONDARY STAR-FORMATION

Sunetra Giridhar
Indian Institute of Astrophysics, Bangalore-560034, India

In addition to the well-known radial abundance gradient in the disc of our Galaxy, there are indications of small-scale variations (Talent and Dufour 1979, Giridhar 1983). We have compiled spectroscopic abundances for long period Cepheids and to eliminate the effect of differences in ages, derived their places of formation by calculating their galactic orbits backwards in time. The stellar orbits were calculated considering the axisymmetric gravitational potential as well as the spiral potential due to the density wave. The parameters related to spiral waves are taken from Yuan (1969). The equations of motion in the (ξ,η,ζ) system were numerically integrated using the Runge-Kutta method and birthsites were transformed to (ξ,η) in the reference frame of the spiral pattern. The details of the computations are described by Giridhar (1985). In addition to the accepted value of 13.5 km s^{-1} kpc^{-1} for pattern velocity, birthsites were also calculated for ω_p = 11.5 and 15.5 km s^{-1} kpc^{-1}. Figure 1 shows the birthsites in the galactic plane for the three values of the pattern velocity. The Cepheids in the figure

TABLE I. Birthsites for the Sample Cepheids

S No.	Star	Fe/H	Birthsite in ω_p System		S No.	Star	Fe/H	Birthsite in ω_p System	
			ξ_p	η_p				ξ_p	η_p
1	UZ Sct	+0.25	3.48	-2.52	12	β Dor	+0.01	0.68	-3.95
2	WZ Sgr	+0.15	2.19	-0.88	13	TX Cyg	+0.39	-0.26	-1.19
3	S Nor	+0.10	2.47	-3.88	14	δ Cep	+0.00	1.51	-4.55
4	SV Vul	+0.28	0.45	+0.75	15	ζ Gem	+0.27	-0.11	-3.77
5	Y Oph	+0.18	0.88	-2.11	16	RT Aur	+0.06	+3.19	-5.77
6	U Sgr	+0.10	1.60	-4.40	17	RS Pup	-0.07	2.20	-4.28
7	W Sgr	+0.27	2.12	-5.34	18	DL Cas	-0.13	-0.91	-1.94
8	X Sgr	+0.05	1.90	-4.68	19	T Mon	+0.10	-0.90	-1.54
9	η Aql	+0.07	1.54	-4.30	20	RX Aur	-0.37	-0.57	+1.49
10	X Cyg	+0.19	-0.62	-1.52	21	SV Mon	-0.10	-1.97	+1.72
11	T Vul	-0.05	1.18	-5.34	22	BM Per	-0.10	-2.74	+0.26
					23	YZ Aur	-0.26	-4.38	+0.57

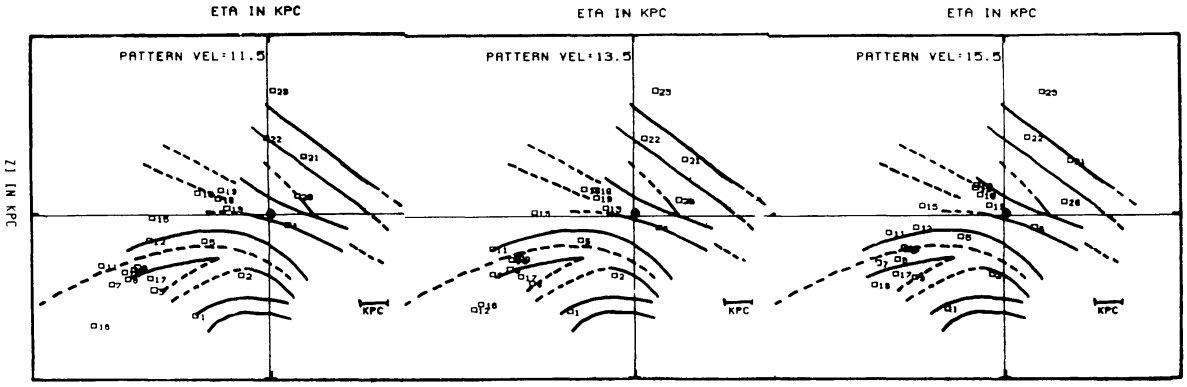

Fig. 1

can be identified through the serial number in Table I which contains our compilation of Fe/H and derived birthsites. It is obvious from the figure that the systematic shifts in birthsites for different pattern velocities are not large enough to affect the assignment of birthsites to different arms.

An interesting trend observed is that the stars born in major spiral arms (Sagittarius and Perseus) yield a shallower abundance gradient of -0.05 dex with a small scatter of ±0.08 dex. Cepheids formed in the local arm and in interarm regions differ from this relation by 0.18 dex in the mean and exhibit a large scatter of 0.25 dex. We suggest that the stars in the minor features are formed via secondary star formation in the ISM enriched by massive stars formed in the main spiral arms. Also this secondary star formation must have taken place before the mixing due to turbulent eddies and differential rotation in the galactic disc could dilute the enrichment of the ISM. These stars would exhibit higher metallicity if the secondary star formation starts about